Effect of Bimodal Powder Mixture on Powder Packing Density and Sintered Density in Binder Jetting of Metals

Yun Bai, Grady Wagner, Christopher B. Williams
Design, Research, and Education for Additive Manufacturing Systems Laboratory
Department of Mechanical Engineering
Virginia Tech
REVIEWED

Abstract

The Binder Jetting Additive Manufacturing process provides an economical and scalable means of fabricating complex metal parts from a wide variety of materials. However, the performance metrics of the resulting sintered parts (e.g., thermal, electrical, and mechanical properties) are typically lower than traditionally manufactured counterparts due to challenges in achieving full theoretical density. This can be attributed to an imposed constraint on particle size and its deleterious effects on powder bed packing density and green part density. To address this issue, the authors explore the use of bimodal powder mixtures to improve the sintered density and material properties within the context of copper parts fabricated by Binder Jetting. The effectiveness of using bimodal powder mixtures in an effort to improve sintered density is studied in terms of particle size distribution and powder packing density.

Key words: Binder jetting, Additive manufacturing, Copper, Sintering, 3D printing, Powder metallurgy

1. Introduction

1.1 Challenges in Binder Jetting of Metals

The Binder Jetting Additive Manufacturing (AM) process can be used to fabricate metal parts by selectively ink-jetting a liquid binding agent into a powder bed, followed by post-process sintering of the printed green part. In the green part creation stage, the binder droplets interact with the powder particles to form primitives that stitch together to form a cross-sectional layer. Once a layer is printed, a new layer of powder is spread by a counter-rotating roller on top of the previous layer which is then printed and stitched to the previous layer by the jetted binder. The layer-by-layer process is repeated to create the complete green part. The unbound loose powder in the bed that surrounds the part supports overhanging structures during the build, and can be removed after printing via compressed air. Once depowdered, the green part is placed in a high-temperature furnace to pyrolyze the binder and sinter the powder particles together through atomic diffusion in order to obtain final density and strength.

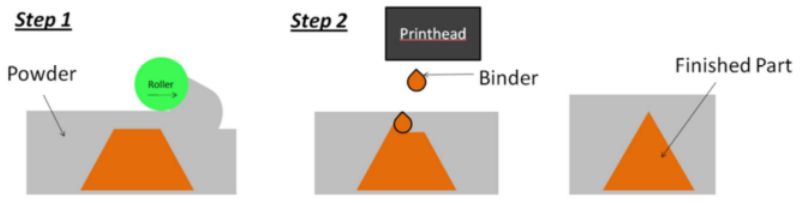

Figure 1. Green part printing process in Binder Jetting

As Binder Jetting of metal functionally separates part creation from powder sintering, the common processing challenges found in direct-metal Additive Manufacturing processes – such as residual stresses imposed by rapid solidification of a melt pool, which lead to part warping and added anchors and/or heat sinks to geometry – are avoided (Mercelis and Kruth, 2006; Mumtaz et al., 2011; Shiomil et al., 2004). The ability to fabricate a part in a powder bed without the need for built anchors enables Binder Jetting to create large, geometrically complex parts without difficult post-process cleaning. Binder Jetting is also an inherently scalable technology as it does not require an enclosed chamber and expensive energy sources. In addition, as Binder Jetting does not use an energy beam to process material, it is well suited for optically reflective and thermally conductive metals, which can be challenging for Powder Bed Fusion processes. For example, the feasibility of manufacturing high purity copper via Binder Jetting on ExOne 3D printers has been demonstrated in the authors' previous work (Bai and Williams, 2015).

The primary challenge in fabricating metal parts using Binder Jetting is in achieving a fully dense product following the sintering post-process. Pores typically exist in sintered ceramics or metals fabricated in Binder Jetting (Chou et al., 2013; Zhang et al., 2014). For example, while the authors were able to create complex structures from gas atomized copper powder, the overall mechanical strength (116.7 MPa) and conductivity is constrained by the parts' substantial porosity (85.5% dense parts). Part porosity is challenging to eliminate during sintering because of a low powder bed density and the inability to process ultra-fine powders. Loosely packed powders have less contacting points and large empty spaces between particles, which reduce available sintering and neck formation sites. The spreading of fine powders can be difficult in powder-based AM processes due to low flowability and powder agglomeration, but the presence of large particles in the powder significantly lowers the driving force for sintering (reduction of surface energy). As such, metal parts made by Binder Jetting are typically infiltrated with an infiltrant material in order to obtain full density.

Pressure assisted sintering provides a viable solution to achieve pore-free density in Binder Jetting of metals. Green parts can be sintered to an initial density and then Hot Isostatic Pressing (HIP) can close the pore as a second treatment. The use of HIP has demonstrated to be able to approach full density in a slurry-based Binder Jetting of tungsten carbide (Kernan et al., 2007). This strategy typically requires a high initial sintered density (usually over 93%) to enable capsule-free HIP so that complex shapes can remain intact. Thus, the goal of this work is to identify processing techniques with a focus on powder for improving sintered density of metal parts created by Binder Jetting to a value that is suitable for HIP.

1.2 Improving sintered density via bimodal powder mixtures

To accomplish the goal of achieving a high initial sintered density, the authors look to the mature Powder Metallurgy (PM) discipline as it is similar to Binder Jetting in that part sintering is separated from green part formation. One well-established theory in Powder Metallurgy to improve powder packing density is to use bimodal powder mixtures. The increased powder packing density in bimodal powder mixtures, wherein the small particles fill the interstitial voids between coarse particles, has many benefits such as improved unfired property and less shrinkage given a certain sintered density. Zheng provides a review of the developed models and

demonstrated importance of the particle size distribution to obtain dense packing (Zheng et al., 1995).

Compared with the certainty and reliable prediction in improving powder packing density, the sintered density improvement by bimodal powder is often complicated and can be unsuccessful. German developed a prediction of sintered density of bimodal mixtures and validated by a series of experiments with various materials (German, 1992). Both models and practices showed the rapid sintering rate and enhanced sintering stress of small particles in sintering (Coble, 1973); however, added smaller particles typically bond to the large particles and offer little influence on the overall densification. The addition of large particles to fine powders may increase the packing density, but it will also hinder densification. In these two cases, a sintering stress develops in the powder mixtures and may inhibit densification, especially at lower sintering temperature and shorter time. As a result, despite a successful increase in powder packing density, many sintering experiments involved with bimodal powder have failed to show a corresponding increase in the sintered density.

Particle size distribution and bimodal mixtures have been explored in some powder-bed AM processes (SLS, SLM, etc.); however, the study of bimodal powder mixtures in the context of Binder Jetting is limited. In Powder Bed Fusion, particle size distribution plays an important role in increasing layer density (Karapatis and Egger, 1999); preventing balling phenomenon and achieving higher radiative heat flux in the powder bed (Zhou et al., 2009); and selecting the optimal printing parameters (Spierings et al., 2010; Spierings and G., 2009). In Binder Jetting, Sachs studied the improved surface finish and printing primitives in unfired parts using bimodal powder distribution (Lanzetta and Sachs, 2003). Verlee explored the sintered density of stainless steel bimodal mixtures with various mixing ratios under one sintering condition. Like many Powder Metallurgy models have predicted, the experimental result did not show an improvement in sintered density by mixing large particles to the fine (Verlee et al., 2011).

1.3 Context

While there is little demonstrated benefit of bimodal mixture in improving sintered density within Powder Metallurgy, the effect of bimodal powder mixture in Binder Jetting of copper is hypothesized to have a different impact on sintered density for the following reasons:

1. The powder bed in Binder Jetting is much less dense than many traditional Powder Metallurgy especially for fine powders. The low packing density is a main obstacle in achieving fully dense parts, which could have a strong impact on sintered density.
2. Binder Jetting of metals typically requires a large sintering temperature and duration, which could facilitate sintering stress relaxation, and thus denser final parts.
3. Sintering behavior is material specific. Copper sinters well in PM contexts; however its study in the context of Binder Jetting is limited.

Beyond improving sintering densification, the use of bimodal mixed powders in Binder Jetting is also expected to bring some additional benefits. As most metal parts in Binder Jetting undergo a large degree of shrinkage after sintering (without infiltration), there is a need to use high packing density powders to reduce shape distortion for a better dimensional control,

especially for high precision parts. In addition, a powder mixture containing coarse powders will have a decreased cost as compared to a powder bed composed of solely fine powders.

This paper describes the authors' efforts to validate the hypothesis that the use of a bimodal powder mixture will improve final part density. This objective is achieved by processing copper parts made various particle size distributions and powder bed densities via bimodal powder mixtures. The authors' experiments explore the effects of adding large/small particles into a base powder on the final sintered density under different sintering conditions. The experimental method is detailed in Section 2. A discussion of the results is presented in Section 3, and closure is offered in Section 4. While the results convey the effects of processing bimodal copper powder, the overall goal of this paper is to develop a fundamental understanding and methodology of material property improvement via powder optimization in Binder Jetting of metals.

2. Experimental Method

2.1 Powder selection and characterization

Powder characteristics such as morphology, size, and distribution affect final part quality. The authors have chosen to use gas atomized powders as they provide excellent packing density and are easily recoated. As an additional benefit, spherical powder requires minimal binder to form necking between particles compared to irregularly shaped particles (Cima et al., 1992).

Many models and experimental results have shown that high packing density can be achieved when the volume fraction of fine powder is between 0.2-0.4 (Zheng et al., 1995). In this paper, bimodal mixtures were created by mixing fine powder (15 μm or 5 μm) with coarse powder (75 μm or 30 μm) with a 73-27 weight ratios in a rotating drum. The powders used for mixing are listed in Table 1. Each mixture was mixed for 2 hours to ensure an even mixture. Laser scattering with a Horiba LA-950 was used to analyze particle size distribution (ASTM B822) of the powder mixtures.

Table 1. Powder description

Powder name	*D10*	*D50*	*D90*	*H_2 Loss%*
75 μm powder	58.0	77.0	101.5	N/A
30 μm powder	15.0	30.0	37.5	0.40
15 μm powder	8.0	17.0	28	0.30
5 μm powder	0.65	5.5	9.0	0.65

2.2 Powder bed analysis

As bimodal mixtures are hypothesized to significantly affect green part density, and in Binder Jetting the green density largely depends on the powder bed density, the authors employed a variety of methods for evaluating powder bed density. Apparent density, which should be the lower density threshold in Binder Jetting, was measured using a Hall flow meter (ASTM Standard 212). Tap density, which should be the upper threshold, was measured using a tapping apparatus

(ASTM Standard 527). The actual powder bed density should be in between the apparent and tap density because of the compaction of the spreader; however, this density is usually difficult to be directly measured. Inspired by some other powder-bed AM processes, in this work a cup was first printed into the powder; powder bed density was then calculated by measuring the mass of powder contained in the cup dividing the cup volume.

Apparent and tap density is convenient to measure and usually comes with high accuracy; therefore these two densities can be used for powder screening in Binder Jetting, especially when packing density is the main concern. In addition, the ratio of apparent and tap density (Hausner ratio) can assess powder flowability – the lower this ratio, the better the flowability. Powder packing characteristics can be assessed by directly measuring the powder bed density with a printed cup or measuring green part density. The printed cup method is preferred as it eliminates the binder effect; however, the measurement can lose its accuracy when ultra-fine powders (non-free flowing) are used as they prove to be difficult to completely remove from the cup.

2.3 Printing process parameters

An off-the-shelf standard metal binder (PM-B-SR2-05) from ExOne was used for all experiments as it leaves minimal binder residue after sintering and is compatible with both the Binder Jetting machine (ExOne R2) and copper powder used in this study. 18mm x 6mm x 3 mm test coupons were printed for characterization of the various powder mixtures.

To ensure successful spreading, the layer thickness must be larger than the largest particle, and it is recommended that the layer thickness should be at least three times the layer thickness to acquire a higher packing density and smoother surface finish (Utela et al., 2008). In addition, the layer thickness cannot be larger than the radius of a primitive to ensure that subsequent layers are bound together. In this paper all samples are printed with an 80 μm layer thickness.

Saturation ratio is the ratio of the amount of void space in the powder bed filled with binder to the total amount of void space. Too much binder will permeate through the powder and bind extra powder, which leads to a green part growth and poor surface finish. However, if saturation ratio is set too low, printed binder will not penetrate deep enough to bind layers, which can cause porosity, anisotropic shrinkage, and part delamination. An accurate binder drop volume measurement was made before each print by jetting a known amount binder droplets onto a testing substrate and measuring the total mass. As the fractional volume of void space is different for each explored powder combination, a unique packing density is entered into the process control software for each bimodal powder, and is based on the powder bed density measurements outlined in Section 2.1. The amount of jetted binder is adjusted accordingly to obtain the predetermined saturation value. Based on the considerations stated above and an observation of the primitive size in each powder, a saturation of 150% is used for the 5 μm powder and 100% for the rest. The 5 μm powder has displayed a small primitive size and large total surface area thus requires extra binder for good bonding.

2.4 Post-processing and sintering

The chosen PM-B-SR2-05 binder typically requires curing at 190 ℃ for 2 hours after printing to increase green part strength. All sintering cycles used in this work feature constant heating/cooling rate (3 ℃/min) and contain an isotherm at 450 °C for 30 min to facilitate binder burn-out. To explore the hypothesized different response of bimodal powder mixtures under various sintering conditions, a full factorial design containing two levels of sintering temperature (1020 °C and 1060 °C) and two levels of sintering time (30 min and 120 min) was used for sintering the printed testing coupons.

To measure sintered density, the immersion method with Archimedes principle was used due to the porosity of the part (ASTM Standard 962). This method is used for samples with surface connected porosity by filling the pores with a known content of oil. Shrinkage is calculated by comparing the green dimensions to the sintered dimensions.

3. Results and Discussion

3.1 Powder bed density, green part density, and flowability of bimodal powder mixtures

Tables 2 summarizes the powder and powder mixtures with a decreasing order of median size, and has shown the apparent/tap density improvement in bimodal mixtures. For example, by introducing a small portion of large particles (30 μm or 15 μm) to the 5 μm powder (powder 9), the apparent densities of the resultant powder beds (powder 7 and 8) have improved by 12.7% and 5.6% and the tap density has improved by 5.6% and 4.9%. The increase in apparent density is higher than that in tap density, which is particularly useful for Binder Jetting as its powder compaction effect is limited. Except for the large particle size ratio powder mixtures (75+15 μm mixture) where a dual peak can be observed in the particle size distribution curve, the powder density increase in most mixtures are achieved by a shifted median size and widened size distribution. The relatively small large-to-small particle size ratio in this work (lower than 6) limited the increase in powder packing density; however it is necessary to keep this ratio small so that no extra-large particles are introduced to the mixtures that will be a detriment to sintering.

The Hausner ratio has shown the improved powder flowability (smaller ratio) in all bimodal mixtures (Table 2). The improved flowability is critical in getting smooth and dense powder layers in the recoating process of Binder Jetting.

Table 2. A summary of the size and density of the powder and bimodal powder mixtures

Mixture number	*Median size (D50)*	*Standard deviation*	*Powder components*	*Apparent density*	*Tapped density*	*Hausner ratio*
1	77.9 μm	23.2 μm	75 μm	56.1 %	64.9%	1.16
2	27.0 μm	39.2 μm	75 μm (w.t.73%)+15 μm	59.7 %	66.9%	1.12
3	26.4 μm	10.9 μm	30 μm	48.5 %	60.8 %	1.25
4	17.4 μm	12.4 μm	30 μm (w.t.73%)+5 μm	53.7 %	63.9 %	1.19
5	17.0 μm	6.7 μm	15 μm	52.9 %	65.1%	1.23
6	10.8 μm	4.7 μm	15 μm (w.t.73%)+5 μm	54.6 %	67.4 %	1.23
7	8.3 μm	15.4 μm	5 μm (w.t.73%)+30 μm	54.4 %	61.2 %	1.13
8	5.8 μm	2.7 μm	5 μm (w.t.73%)+15 μm	47.3 %	60.5 %	1.28
9	5.5 μm	N/A	5 μm	41.7 %	55.6 %	1.33

Both green density and estimated powder bed density can be used as an indication of powder packing density improvement in bimodal powder mixtures. In Figure 2, the value of powder bed density (obtained by measuring powder in a printed cup; Section 2.2) is measured as in between of apparent density and tap density in each powder. The powder bed density is more similar to the apparent density for fine powders, while it is more similar to the tap density for high flowability powders (75 μm and 30 μm). Figure 2 also compares the green density with the apparent and tap densities of selected powder mixtures. The green density of the printed parts is slightly lower than the apparent density for most powders (except for powder 9). This is believed to be caused by the binder spread effect at the edge of the printed parts that glues extra powder particles, which result in a green part dimensional expansion over the original design.

All density measurement methods have shown noticeable increases in powder density in the printed parts. In Figure 2, it is seen that a better powder bed density is achieved by either mixing small particles (5 μm) or mixing large particles (75 μm) into the 15 μm powder, with an increase of 5.7% and 16.2% respectively. Figure 2 also shows that the mixtures containing 5 μm powders improve the green density by 3.0%-9.4% when compared to the pure 5 μm powder. This result shows a means for increasing powder bed density while still retaining most of the fine powders, which are important for sintering performance.

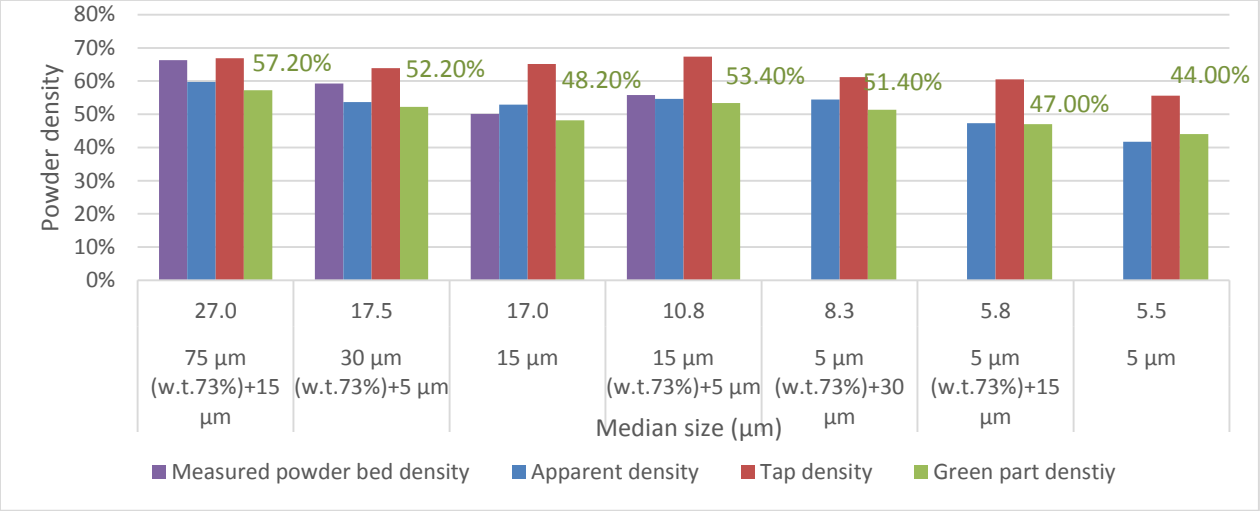

Figure 2. Comparison of apparent density, tap density, green density (with density numbers shown in the graph), and measured powder bed density (only for the coarse powders to ensure measurement accuracy) in Binder Jetting

3.2 Packing density and particle size effect on sintering

To explore the effects of bimodal mixtures on part densification during sintering, a non-mixed powder (15 µm) and three powder mixtures (15 µm+5 µm powder, 75 µm+15 µm powder, 30 µm+5 µm powder) were printed into testing coupons and sintered. The mixing ratio was held constant for this section (73% coarse powder). As noted in Section 3.1, compared with the 15 µm powder, the 15 µm+5 µm powder introduces fine particles into the mixture and has increased powder bed density by 5.7%; the 75 µm+15 µm powder brings large particles into the mixture and has improved the powder bed density by 16.2 %.

Samples were printed using the same printing parameters as described in Section 2.3. The isotherm temperature and time in the sintering heating schedule was varied at two levels (1020 °C and 1060 °C, and 30 minutes and 120 minutes), as indicated in Figure 3. In each quadrant, the sintered density (lower section) and densification (upper section) of each sintering cycle are compared across the powder mixtures. The densification is represented by the density gain from powder bed density to sintered density.

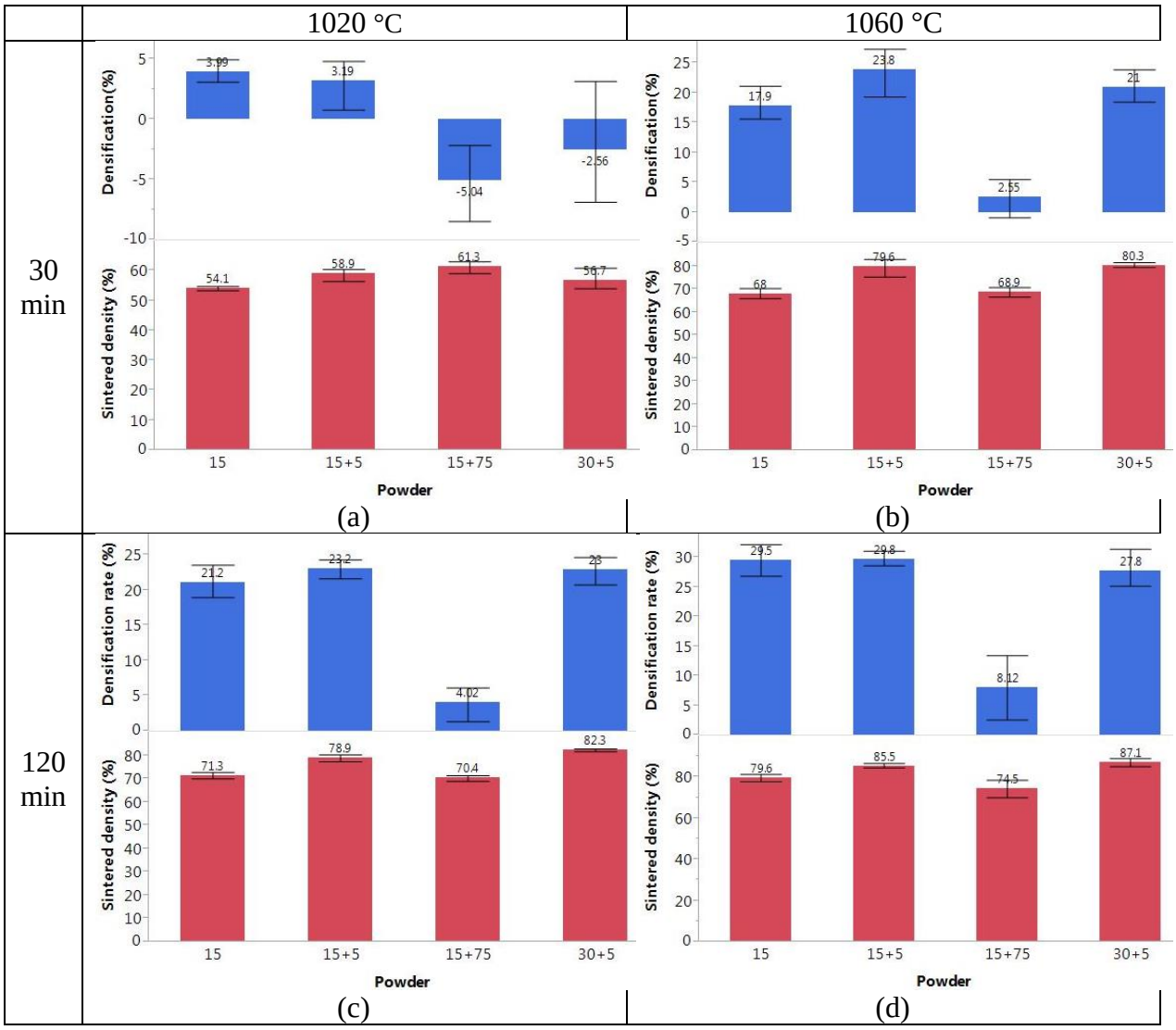

Figure 3. Sintered density and densification comparison across the powder under various sintering conditions

The parts sintered under the least sufficient sintering condition (1020 °C for 30 minutes) achieved less densification than higher isotherm temperatures and longer holds. In addition, Figure 3 (a) shows that when large particles are present in Binder Jetting (75+15 µm and 30+5 µm powder mixtures), the sintered density can be lower than the powder bed density (the parts still densified as the actual green density is lower than the measured powder bed density). Under this condition, powder bed density still plays an important role in determining sintered density as the sintering densification is limited.

An increase in powder bed density by introducing extra-large particles has failed to effectively improve the sintered density. This is demonstrated by comparing the 75+15 µm powder mixture with the 15 µm powder in Figure 3(b), (c) and (d). Figure 4(b) shows the necking has a tendency to form between 15 µm and 75 µm particle. There is limited sign of direct necking and merging of 75 µm particles due to the large particle radii. The sintered part is composed of a rigid skeleton of 75 µm particles, wherein the sintering of fine powders have little

contribution to the overall densification. This phenomenon is not alleviated by the sintering temperature studied in this work. This result is similar to what has been found in traditional Powder Metallurgy (German, 1992).

From these results, it is clear that an increase in powder bed density without shifting median particle size is an effective method to improve sintered density. This is demonstrated by comparing the 30+5 μm powder mixture with the 15 μm powder. Compared with the 15 μm powder (median size of 17.0 μm), the 30+5 μm powder mixture has a very similar median particle size (17.4 μm) but a wider distribution, which results 9.2% higher powder bed density. This difference results in a 7.5%-11.7% sintered density depending on the sintering condition (Figure 3).

The highest sintered density (87.1%) occurred in 30+5 μm powder samples when sintered at 1060 °C for 120 minutes. The powder mixture provides more contact point as available neck formation sites, thus small particles are able to "glue" neighboring large particles and form an integrated structure by surface reduction (Figure 5). Despite the significant increase in sintered density, the volumetric shrinkage in 30+5 μm powder only increased by 2.4% than in the 15 μm powder (Figure 6), which is another benefit of powder mixing. The linear shrinkage is anisotropic but displays a similar trend.

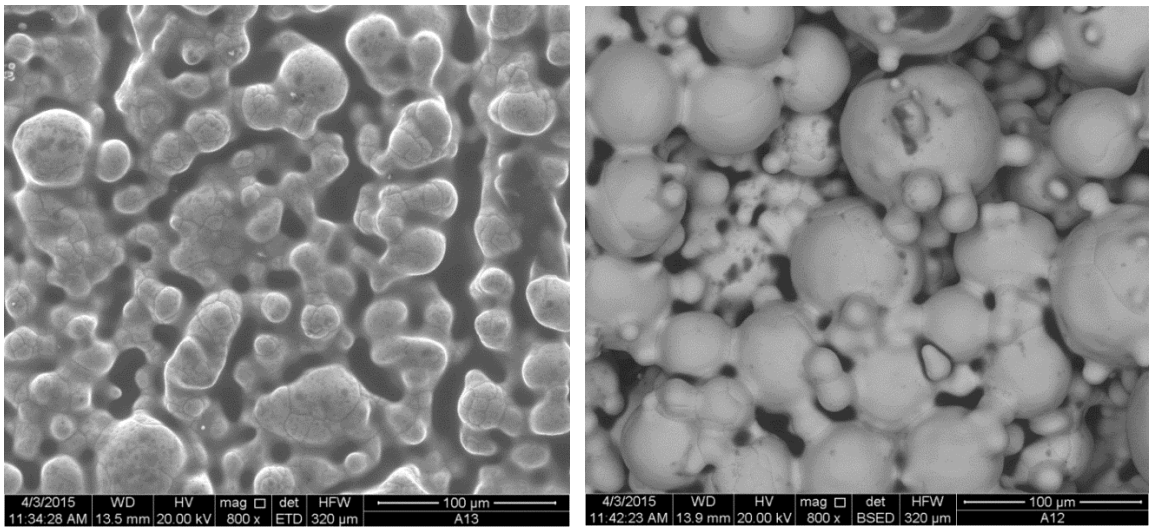

(a) **(b)**

Figure 4. Sintered structures of the primitives in (a) 15+5 μm powder and (b) 75+5 μm powder, sintered at 1060 °C for 120 minutes

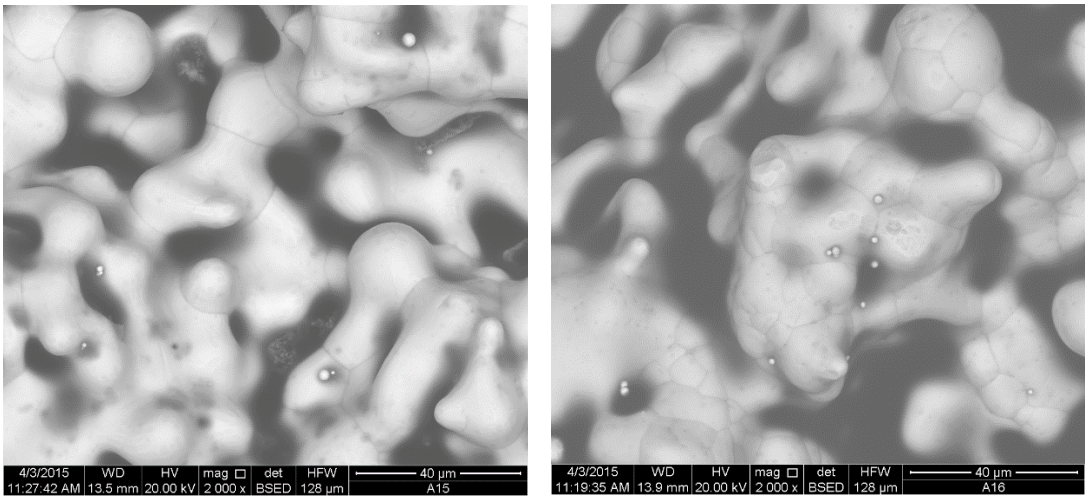

(a) (b)

Figure 5. Sintered structures of the primitives in 30+5 µm powder, sintered at 1060 °C for 120 Minutes

Similarly, the mixing of 5 µm powder into 15 µm powder is capable of increasing sintered density as both powder bed density and particle size is improved. 15+5 µm powder has the highest density gain among the powders tested as it has the smallest median size. Like 30+5 µm powder, interconnected sintered agglomerates are observed in Figure 4(a).

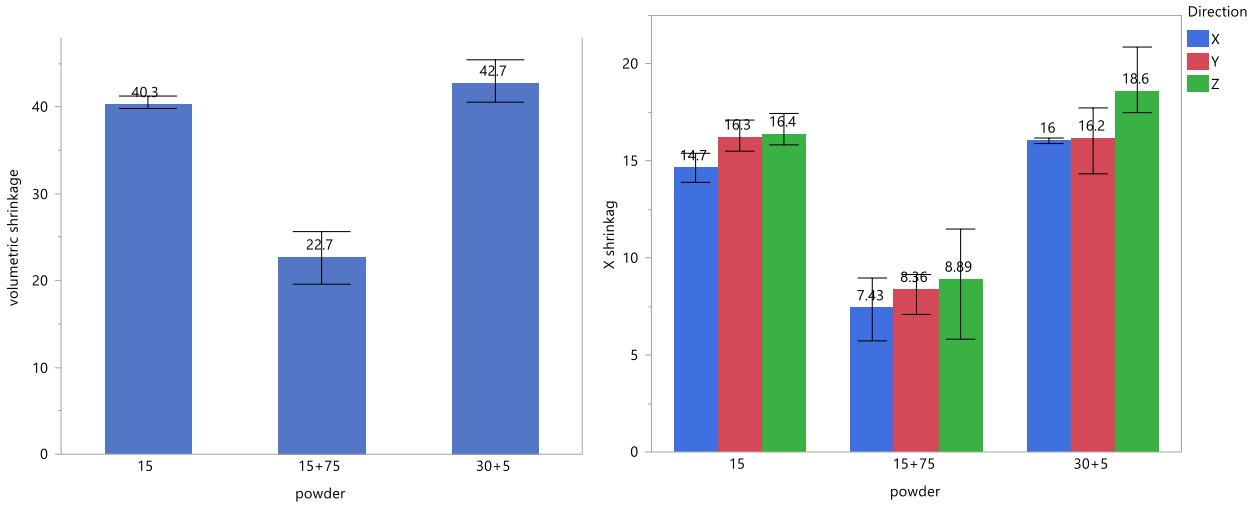

(a) (b)

Figure 6. (a) Volumetric shrinkage and (b) X, Y and Z linear shrinkage of the powders sintered at 1060 °C for 120 minutes

4. Conclusion

The bimodal powder mixtures in the context of Binder Jetting of copper is capable of improving spreading, powder bed density, and sintered density compared with the constituent powders.

The strategy of increasing powder bed density and flowability via bimodal powder mixtures is particularly effective for Binder Jetting. By adopting bimodal powder mixtures, the powder flowability is improved by up to 15% (30+5 µm powder; Section 3.1). Despite the relatively small particle size ratio (3-6 when 15 µm powder or 30 µm powder is mixed with 5 µm powder) used in this work, the powder bed density is able to be improved by up to 16.2% (Section 3.1). However this dramatic increase in the powder bed density has failed to improve the sintered density when large particles (75 µm powder) are present as they formed a rigid skeleton which limited the contribution of fine powders to overall densification. Widening particle size distribution while not shifting median particle size via bimodal mixtures (e.g., 30+5 µm powder) has demonstrated to be a viable strategy and has shown an increase of sintered density up to 12.3 % depending on the sintering condition (Section 3.2).

This work provides a framework for powder optimization in terms of achieving high sintered density in Binder Jetting of bimodal metal powders. The authors look to explore the effects of different printing parameters and optimize sintering profiles on final part density in future work.

5. Acknowledgement

This material is based upon work supported by the National Science Foundation under Grant No. #1254287. Any opinions, findings, and conclusions or recommendations expressed in this material are those of the author(s) and do not necessarily reflect the views of the National Science Foundation. The authors acknowledge technical support provided by the ExOne Co. The authors also would like to thank NCFL of Virginia Tech, Dr. Carlos Suchicital and Jeremy Beach for their assistance. Special thanks to Dan Brunermer (ExOne Co.) and Joe Strauss (HJE Co.) for the insight on Binder Jetting and Powder Metallurgy.

6. Reference

Bai, Y. and Williams, C.B. (2015), "An exploration of binder jetting of copper", *Rapid Prototyping Journal*, Vol. 21 No. 2, pp. 177–185.

Chou, D.T., Wells, D., Hong, D., Lee, B., Kuhn, H. and Kumta, P.N. (2013), "Novel processing of iron-manganese alloy-based biomaterials by inkjet 3-D printing", *Acta Biomaterialia*, Acta Materialia Inc., Vol. 9 No. 10, pp. 8593–8603.

Cima, M.J., Lauder, A., Khanuja, S. and Sachs, E. (1992), "Microstructural Elements of Components Derived From 3D Printing", *Solid Freeform Fabrication Symposium*, pp. 220–227.

Coble, R.L. (1973), "Effects of Particle-Size Distribution in Initial-Stage Sintering", *Journal of The Ameican Ceramic Society*, Vol. 56 No. 9, pp. 461–466.

German, R.M. (1992), "Prediction of sintered density for bimodal powder mixtures", *Metallurgical Transactions A*, Vol. 23 No. 5, pp. 1455–1465.

Karapatis, N. and Egger, G. (1999), "Optimization of powder layer density in selective laser sintering", *Proc. of the 9th Solid …*, pp. 255–264.

Kernan, B.D., Sachs, E.M., Oliveira, M. a. and Cima, M.J. (2007), "Three-dimensional printing of tungsten carbide-10 wt% cobalt using a cobalt oxide precursor", *International Journal of Refractory Metals and Hard Materials*, Vol. 25 No. 1, pp. 82–94.

Lanzetta, M. and Sachs, E. (2003), "Improved surface finish in 3D printing using bimodal powder distribution", *Rapid Prototyping Journal*, Vol. 9, pp. 157–166.

Mercelis, P. and Kruth, J.-P. (2006), "Residual stresses in selective laser sintering and selective laser melting", *Rapid Prototyping Journal*, Vol. 12 No. 5, pp. 254–265.

Mumtaz, K., Vora, P. and Hopkinson, N. (2011), "A Method To Eliminate Anchors/Supports From Directly Laser Melted Metal Powder Bed Processes", *Solid Freeform Fabrication Symposium*, pp. 55–64.

Shiomil, M., Yamashital, T., Osakada, K., Shiomi, M., Yamashita, T., Abe, F. and Nakamura, K. (2004), "Residual Stress within Metallic Model Made by Selective Laser Melting Process", *Annals of the CIRP*, Vol. 53 No. 1, pp. 195–198.

Spierings, a B., Herres, N., Levy, G. and Buchs, C. (2010), "Influence of the particle size distribution on surface quality and mechanical properties in additive manufactured stainless steel parts", *Solid Freeform Fabrication Symposium*, pp. 397–406.

Spierings, A.B. and G., L. (2009), "Comparison of density of stainless steel 316L parts produced with selective laser melting using different powder grades", *Solid Freeform Fabrication Symposium*, Austin, TX, pp. 342–353.

Utela, B., Storti, D., Anderson, R. and Ganter, M. (2008), "A review of process development steps for new material systems in three dimensional printing (3DP)", *Journal of Manufacturing Processes*, Elsevier Ltd, Vol. 10 No. 2, pp. 96–104.

Verlee, B., Dormal, T. and Lecomte-Beckers, J. (2011), "Properties of Sintered Parts Shaped by 3D-Printing from Bimodal 316L Stainless Steel Powder Mixtures", *Euro PM2011*, pp. 357–362.

Zhang, S., Miyanaji, H., Yang, L., Ali, A. and Dilip, J.J.S. (2014), "An Experimental Study of Ceramic Dental Porcelain Materials Using A 3D Print (3DP) Process", *Proceeding of Solid Freeform Fabrication (SFF) Symposium*, pp. 991–1011.

Zheng, J., Carlson, W.B. and Reed, J.S. (1995), "The packing density of binary powder mixtures", *Journal of the European Ceramic Society*, Vol. 15, pp. 479–483.

Zhou, J., Zhang, Y. and Chen, J.K. (2009), "Numerical simulation of laser irradiation to a randomly packed bimodal powder bed", *International Journal of Heat and Mass Transfer*, Elsevier Ltd, Vol. 52 No. 13-14, pp. 3137–3146.